EAI Endorsed Transactions
on Scalable Information Systems Research Article **EAI.EU**

Optimization of Pointer Meter Recognition

Xinghui Wang[1,2*], Zhenhua Jia[1], Qichao Zhao[2], Liyuan Liu[1]

[1]School of Computer Science and Engineering, North China Institute of Aerospace Engineering, Hebei Langfang, 065000, China
[2]Hebei Space Remote Sensing Information Processing and Application Collaborative Innovation Center, Hebei Langfang, 065000, China

Abstract

In this study, a pointer meter recognition system (PMRS) is designed based on improvement Hough transform algorithm. PMRS offers three advantages in processing captured images: first, adaptive shooting distance, PMRS can adapt to any shooting distance—whether short or long—between the camera and the dial; second, adaptive shooting angle, PMRS can also adapt to any angle between camera and dial; the third, high computational efficiency, the experimental result showed that, PMRS has almost twice the computational efficiency than the general Hough transform algorithms based on multi-resolution. The above three advantages of PMRS are achieved through the following two methods. For the first, adopting the dynamic gain value of the voting mechanism to reduce invalid or redundant calculations in Hough transform which is based on multi resolution mechanism. The combination of variable gain value of the voting mechanism and multi resolution mechanism make PMRS adapt any shooting distance and high computational efficiency. The second, two theorems proposed in this paper, which make PMRS has the advantages of adaptive shooting angle. Theorem 1 proves that the left-right position relationship between any two points in an image has the characteristic of rotational invariance. Theorem 2 proves the consistency between the rotation angle of any vector in an image and the rotation angle of the image. So, Theorem 2 ensures the theoretical feasibility of the improved algorithm, and Theorem 1 provides implementation methods and principles for improved algorithms. Therefore, PMRS can recognize pointer meter without being affected by the angle of image capture.

Keywords: Pointer Meter Recognition, Hough Transform, Rotation Correction, Vector Computing, Computer Visio

Received on 19 November 2026, accepted on 30 August 2026, published on 24 September 2026

Copyright © 2026 Xinghui Wang *et al.*, licensed to EAI. This is an open access article distributed under the terms of the CC BY-NC-SA 4.0, which permits copying, redistributing, remixing, transformation, and building upon the material in any medium so long as the original work is properly cited.

doi: 10.4108/eetsis.10989

*Corresponding author. Email: wangxinghui@nciae.edu.cn

1. Introduction

Instrument recognition algorithm is a technology based on computer vision. This algorithm is used for automatic analysis and identification of various indications and parameters on instruments. Instrument recognition algorithms have wide applications in industrial automation, energy management, environmental monitoring, and other fields. The pointer type meter still has much application in industry and consumer use [1][2]. According to the data display form, it can be classified into two types: the pointer type and the pointer-wheel combination. Unlike electronic meters, the data from pointer meters require manual interpretation [3]. Modern industry has promoted the development of electronic meters, but this does not diminish the usefulness of analogue point meters. Electronic meters are commonly used in both industrial production and daily life, owing to their accuracy and lower cost, among other reasons. The traditional pointer meter, in contrast, is costly, inefficient, and prone to errors. Capturing the meter's image, and the pattern recognition technology used to identify the data from pointer meter, have become the most important foci of the pointer meter's related application [4][5][6][7]. The pointer meter recognition algorithm proposed by the paper is based on Hough Transform algorithm. The essence of Hough transform algorithm is to calculate the parameter information of the target by voting mechanism [8][9] and then detect the specific target from the image. Hough transform was originally used to detect the straight line in the image, then it was extended to recognize objects in any shape, such as circle, ellipse or curve. Hough transform is widely used in the field of pattern recognition for its good anti-noise performance and insensitivity to partial occlusion of the target to be detected.

The basic processing flow of the instrument recognition algorithm based on computer vision and pattern recognition technology is as follows [10].

- Image acquisition, using image acquisition equipment to obtain images of instruments.
- Image preprocessing, which preprocesses the collected images, including denoising, filtering, graying, binarization, and other processing techniques, to achieve the goal of improving image quality [11].
- Feature extraction, extracting feature information of instrument indicator parameters from preprocessed images, such as shapes, edges, feature group points, etc.
- Feature matching, matching the extracted features with model parameters to determine the type, location, and other information of the instrument
- Parameter interpretation: Based on the identified feature data, relevant algorithms are used to interpret various indicators and parameters on the instrument, such as flow rate, pressure, etc.

The first part of this paper introduces the Hough transform and improvements made to the algorithm to make it more efficient. The second part of this paper introduces the identification algorithm for the pointer dial, including the principle of the algorithm revised by the group. The third part describes the calculation method for the dial's rotation angle and its correction method, which makes the algorithm adaptable to any angle within 360 degrees. The fourth part shows the computational efficiency and data analysis of the PMRS designed by the group. The fifth part summarizes and evaluates the advantages and disadvantages of the pointer meter recognition algorithm proposed by the group.

2. Recognition of Pointer Meter Dial

Introduction to Hough transform

According to the principle of dot-line duality, the Hough transform can detect a straight line or parts of a straight line in an image [12][13].

Using the transformation of the dot-line duality principle, the Hough transform can be used to detect the circles in an image, and in this study, it was used specifically to detect the circle of the pointer-type dial using the formula shown in Equation 1.

$$(P_x - O_x)^2 + \left(P_y - O_y\right)^2 = R^2 \tag{1}$$

In Equation 1, P is any point on the circumference, O is the center of the circle, and R is the radius of the circle. When a circle is to be detected using the Hough transform, the basic parameters for voting calculation are the center of the circle O and the radius of the circle R. Three essential points should be noted when the Hough transform is used in engineering; they are as follows:

(1) Because the image data are discrete points, radius R should float within a certain range and not be a fixed value, so points that are close to circumference should be considered as points on the circumference and participate in the voting calculation of the Hough transform. Using this appropriate transformation, Equation 1 can be transformed into Equation 2

$$\left|(P_x - O_x)^2 + \left(P_y - O_y\right)^2 - R^2\right| \leq \varepsilon \tag{2}$$

(2) According to the principle of the Hough transform, each point in the image will be calculated as point O in Equation 2. Therefore, the point on one circumference of the circle can be calculated according to Equation 2. The Hough transform must be done for each point in the image, so when the detection position is changed, the point on the circumference can be obtained by translating the calculated data instead of repeatedly calculating the position of the point on the circumference for each new circle.

(3) A difference in snapping distance will result in a different size of the dial in the image. To recognize the position of the dial adaptively, the Hough transform must be done for circles of different radii to obtain the optimal solution. Under these circumstances, we must consider using the Hough transform algorithm based on multi-resolution [14][15] to advance its computational efficiency.

3. Improvement of Hough transform

When the group used the Hough transform to recognize the dial, the group optimized the Hough transform algorithm based on a multi-resolution mechanism. First, under low resolution conditions, we use the Hough transform to match the dial by different given radii. At this time, the image resolution is low, and the data involved in the Hough transform are few, so the algorithm has high computational efficiency. Second, after the dial radius R and position O parameters are obtained, the original resolution of the image is restored, and the Hough transform is used again to recognize the position of the dial in the dial area of the image more accurately. The improved Hough transform in PMRS is not limited to circle detection alone but serves as a foundational localization framework for multiple geometric features in pointer meter recognition. The algorithm first detects the dial boundary through circle parameter voting, and the obtained geometric constraints are then reused for pointer localization, angle correction, and reading extraction. By performing multi-stage feature detection under constrained parameter space, the algorithm improves robustness against variations in shooting distance and viewing angle while maintaining computational efficiency. At this time, although the image resolution is high, the data involved in the Hough transform are reduced from the whole image to the area just around the dial, so the Hough transform is still small. Therefore, the improved algorithm has high computational efficiency.

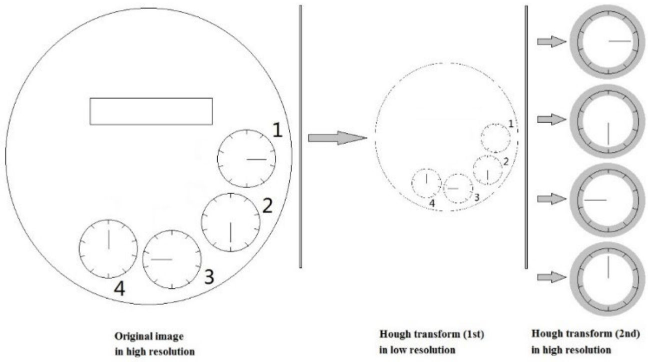

Figure 1. Improved Hough transform based on multi-resolution

The gray area on the right side of Figure 1 shows the possible fluctuation range of the dial's diameter when the Hough transform is used to detect it.

Compared with the general Hough transform based on multi-resolution, the improved algorithm has the following advantages.

First, the improved Hough transform algorithm has high computational efficiency.
The calculation formula for the number of times (N)of calculation when the Hough transform is used to detect a circle is as follows:

$$N = a \times b \times c \times d \tag{3}$$

a: total number of pixels based on image resolution.
b: the circumference data for the dial to be detected by the Hough transform.
c: gain; the number of pixels involved in the Hough transform is between one and three times the number of pixels on the circumference, and c represents this multiplier.

d: the number of times the Hough transform should be called. When the Hough transform is used to recognize circles, it is necessary to perform the transform multiple times to adapt to different radii.

The group improved the Hough transform algorithm by reducing the gain, which improved the computational efficiency, using the specific method described as follows.

In the voting mechanism of Hough transform, the calculation of voting coordinates involves rounding errors and model errors. Rounding error is mainly caused by the process of calculating projection coordinates by rounding floating point numbers to positive integers, while model error is mainly caused by the need for redundant data on certain boundaries in the detection of specific graphics. These redundant data are mainly caused by the parameter ‘ ε ‘in formula (2), and the larger the value of ' ε ', the more redundant data there is. Reducing these redundant data is the key to further optimizing the algorithm. The group has made certain modifications to formula (2) to minimize model error. The improved form of formula (2) is as follow.

$$(P_x - O_x)\cos\theta + (P_y - O_y)\sin\theta = R \tag{4}$$

In formula (3) θ and R are 2 voting parameters of Hough transform. Due to the removal of the square term in formula 2, formula 3 no longer amplifies the error range. Therefore, the improved algorithm by our research group ignores the model error, that is, the parameter ‘ ε ' in formula (2) is ignored.

Taking a 640px×480px image as an example, with a dial diameter of about 80 pixels and a 16-pixel fluctuation range, the gain coefficient was initialized as 2. In practice, the gain coefficient is usually set between 3 and 4; here, it was set to 2 to facilitate statistics.

The number of calculations required by the general Hough transform to detect the dial circle is approximately 1,800,000,000 times. The statistical process of the calculation steps is as follows:

$$\sqrt[a]{(640-80)\times(480-80)} \times \sqrt[b]{80\times\pi} \times \sqrt[c]{2} \times \sqrt[d]{16} \approx 1800000000$$

The number of calculations required by the general Hough transform based on multi-resolution (quarter zoom, i.e. 1/4 of the original image) to detect the dial is about 112 000 000. The statistical process of the calculation steps is as follows:

$$\sqrt[a]{((640-80)/2)\times((480-80)/2)} \times \sqrt[b]{(80/2)\times\pi} \times \sqrt[c]{2} \times \sqrt[d]{(16/2)} \approx 112000000$$

The number of calculations required by our revised Hough transform to detect the dial is about 57 000 000. The statistical process of the calculation steps is as follows.

$$\overbrace{[(640-80)/2 \times (480-80)/2]}^{a} \times \overbrace{[80/2 \times \Pi]}^{b} \times \overbrace{2/2}^{c} \times \overbrace{[16/2]}^{d} + \overbrace{[(80+16-80)^2]}^{a} \times \overbrace{[80 \times \Pi]}^{b} \times \overbrace{[2]}^{c} \times \overbrace{[16/2]}^{d} \approx 57000000$$

From these analysis results, the demonstrated computational efficiency of our revised algorithm is doubled by reducing the value of the gain coefficient. This method sacrifices accuracy in exchange for higher computational efficiency.

Second, the improved Hough transform algorithm is highly accurate. Because the improved Hough transform algorithm is calculated in two steps, first at low resolution and then at high resolution, it avoids the trade-off of high accuracy and high resolution.
In PMRS, the improved Hough transform reduces the parameter search space by introducing adaptive geometric constraints and staged feature localization. Since the dial region is first constrained before pointer extraction, unnecessary parameter voting is avoided and the effective computational complexity is reduced to approximately **O (N × k)**, where k is a constrained local search factor ($k << R \times \theta$). Therefore, the improved Hough transform theoretically reduces computation while maintaining recognition accuracy, which explains the experimentally observed acceleration in pointer meter recognition.

Macroscopically, the algorithm reduces the gain coefficient and improves computational efficiency by reducing recognition accuracy; microscopically, the algorithm increases the gain coefficient and improves the calculation accuracy, but the amount of data involved in the calculation has been greatly reduced, which has little impact on the calculation efficiency.

4. Identification of Dial Scale

The principle of scale recognition for the pointer meter is relatively simple. According to the upper and lower limit values of the dial—such as 0–9 for a water meter—the scale intervals can be converted into angle intervals, and then the measurement indicated by the dial pointer is obtained according to the angle of the dial pointer. The relationship between the dial scale and the pointer angle is shown in Figure 2.

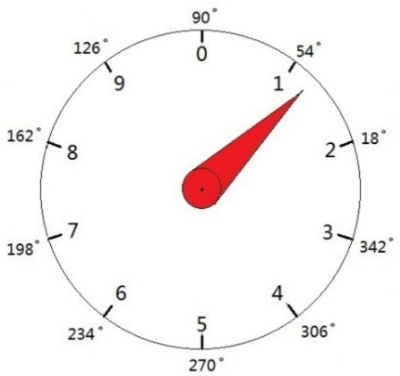

Figure 2. Dial scale and pointer angle diagram

When the position of the dial circle is obtained using the Hough transform, the position of the center O is obtained too. After the image is processed in a special way, such as with threshold filtering [16]], HSI classification [17][18], or feature extraction [19], only the pointer remains in the image. At this time, the geometric center P of the pointer image can be calculated, and the pointer direction can be determined by either OP or by making use of the least squares method to fit the pointer line in the image [20][21][22]. The scale of the pointer can then be calculated by applying the above principle.

In some cases, the dial detection can be done without the Hough transform algorithm [23-24]. For an example image edge technology can be used to process the dial image, but this method does not involve dial detection and positioning technology. In reference [25], a canny operator is used to detect the edge of the dial circle, but this method is applicable only to the case of a single dial; for instruments with multiple dials, this method cannot locate the position of each sub dial.

5. Calculating Rotation Angle of Dial and Correcting Recognition Result

Judgment of the order of pointer type dials

Vector computing is widely used in image processing. For specific pattern recognition, one image can be described accurately by the key vector information it contains [26][27][28]. In practical image acquisition, small displacement errors may occur in the detected dial center coordinates due to noise, edge discontinuity, or imperfect circle localization. Let the center displacement be represented as $(\Delta x, \Delta y)$. Such deviations introduce minor perturbations in vector-based angle computation; however, when the displacement remains within a small tolerance relative to the dial radius, the resulting angular deviation remains limited. The angular error can be approximately expressed as $\Delta\theta \approx \arctan(\sqrt{(\Delta x^2 + \Delta y^2)}/R)$, where R denotes the dial radius. Since the displacement error is typically much smaller than the dial radius in PMRS, the influence on rotation angle correction remains within acceptable numerical tolerance, thereby preserving recognition stability.

The judgment of the left-right position relationship of two points in a plane can be stated as the following theorem:

THEOREM 1 On a rectangular coordinate plane, let point O be an observation point, and let two orthogonal vectors OA and OB start from point O. If one of the following inequalities is valid, vector OA is to the left of vector OB:

$$\mathrm{OA.x} \cdot \mathrm{OB.y} < 0 \quad \mathrm{OA.y} \cdot \mathrm{OB.x} > 0 \tag{5}$$

Proof:
As shown in Figure 3, let us assume that vector OA is on the left side of vector OB in a counterclockwise fashion. According to geometry, the coordinates of vector OA and vector OB on the X and Y axes are expressed as follows.

$$A_x = OA \cdot \cos\theta$$
$$A_y = OA \cdot \sin\theta$$
$$B_x = OB \cdot \sin\theta$$
$$B_y = -OB \cdot \cos\theta$$

Therefore,

$$OA_x \cdot OB_y = OA \cdot \cos\theta \cdot (-OB \cdot \cos\theta) = -OA \cdot OB \cdot \cos^2\theta \leq 0 \quad (6)$$

$$OA_y \cdot OB_x = OA \cdot \sin\theta \cdot OB \cdot \sin\theta = OA \cdot OB \cdot \sin^2\theta \geq 0 \quad (7)$$

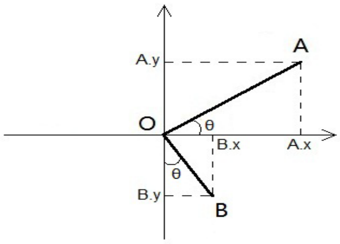

Figure 3. Schematic diagram of two vectors

As shown in Figure 3, in the four quadrants of the Cartesian coordinate system, the vectors OA and OB satisfy Equation 5 and Equation 6 regardless of how the graphic AOB is rotated. Thus, the following conclusions can be obtained:

When $OA_x \cdot OB_y < 0$ vector OA is located to the left of vector OB, while point O is taken as the observation point.

When $OA_y \cdot OB_x > 0$, vector OA is located to the right of vector OB, while point O is taken as the observation point.

In addition, when the product of vector OA and vector OB is zero, the two vectors can be rotated by any angle, such as 30 degrees, and the above judgment is still valid.
(End of proof.) Pointer meter images may be captured under oblique camera viewpoints, resulting in perspective projection distortion. Under moderate perspective transformation, the relative geometric ordering of key dial features remains preserved after projective mapping, although shape proportions may change. Therefore, the left-right positional judgment in Theorem 1 continues to depend primarily on relative coordinate orientation rather than absolute Euclidean distance. Since PMRS further performs rotation angle correction and dial rectification before positional judgment, the effect of perspective distortion is reduced, ensuring dependable left-right discrimination for practical oblique meter viewpoints.

CONSEQUENCE 1 On the Cartesian coordinate plane, let O be the observation point, and let two vectors OA and OB start from point O. If vector OA is located to the left of vector OB, inequality (1) and inequality (2) are both valid.

Proof: This consequence can be proven by Formula (3) and Formula (4) in Theorem 1.
This is a simple conclusion, which can be used to determine the left and right position relationships between multiple recognition targets in the pattern recognition algorithm.

Back to the problem of meter recognition: after the four dials are identified, the left and right position relationships of the sub dials—four example dials in this paper—need to be determined. Since the sub-dial positions given by the Hough transform algorithm are sorted by voting results, they need to be resorted in a clockwise order so we may calculate the calibration value of the meter. The location of the sub dials in the desired order is shown in Figure 4.

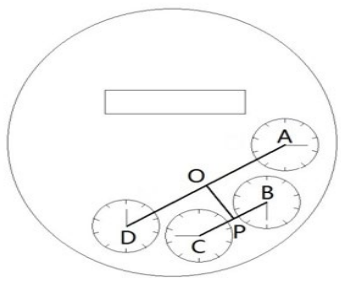

Figure 4. Schematic diagram of the auxiliary vector OP in pointer

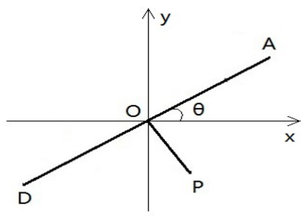

Figure 5. Schematic diagram of the dialin geometric coordinates

According to common sense, the lines drawn between the centers of dials A and D and the dials B and C are two parallel or approximately parallel lines, so dials A and D can be distinguished from dials B and C by a simple vector calculation.

In addition, it is necessary to determine the positional relationship between dials A, B, C, and D. Considering that the camera may be used to take an image from any angle, dial A and dial D may not appear at the same position and angle as shown in Figure 4. Their position and angle are random, but the left-right positional relationship of dials A and D does not change no matter what angle the image is taken from. Dial B and dial C also have these characteristics.

Let the midpoint of dial A and dial D be named O, and let the midpoint of dial B and dial C be named P. We connect OP to make an auxiliary line, as shown in Figure 5. Note that AD and BC are parallel lines. This is key information to determining the combination of AD and BC.
Now, let the center of the rectangular coordinate system be translated to point O. At this time, according to Theorem 1, the left-right positional relationship between point A and point D can be determined. Similarly, the left and right positional relationship between point B and point C can also be determined.

This method can be extended to confirm the left-right relations between two points. The schematic diagram is shown in Figure 6.

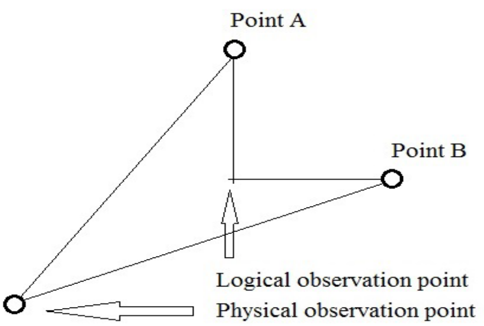

Figure 6. Schematic diagram to confirm left-right relationship of two points

Image rotation

After the left-right positional relationship between the sub dials is determined, the rotation angle of the image can be determined according to the rotation angle of the straight-line AD, as is shown in Figure 7. When pictures of dials are taken in different positions, there is a question of whether the image rotation angle caused by taking photos has an equal effect on the rotation of any straight-line AD in the image. If the effect is the same, the rotation angle of the image can be corrected by the straight-line AD which can be compared with the line AD in the standard image. Theorem 2.1 proves this.

Considering the uncertainty of the captured image angle, it is necessary to calculate the rotation angle of the captured image relative to standard image in engineering.

THEOREM 2 If a plane rotates at an angle α along any axis, the angle for each line's rotation along that axis is α.

Proof: The Cartesian coordinate system can be established with any point as the center that the plane rotates around. The origin of the coordinate system is marked as point O.

As shown in Figure 7, L represents any straight line on the plane. Starting from point O, a perpendicular line to the straight-line L on the plane is first drawn, and the intersection point of this perpendicular line and L is marked as point P. Starting from point P, line segment PA and line segment PB are equidistant along L and can be connected back to O to form isometric triangles the left and right sides of the perpendicular line. Because the length of PA is equal to that of PB, the length of line segment OA is equal to the length of OB. Note that the angle between OA and the X axis is φ, and the angle between OB and the X axis is θ.

Therefore, the polar coordinates of point A are$(OA \cdot \cos\phi, OA \cdot \sin\phi)$. The polar coordinates of point B are$(OB \cdot \cos\theta, OB \cdot \sin\theta)$. If the rotation angle of the plane around point O is α, the polar coordinates of point A become$(OA \cdot \cos(\phi+\alpha), OA \cdot \sin(\phi+\alpha))$. The polar coordinates of point B become $(OB \cdot \cos(\theta+\alpha), OB \cdot \sin(\theta+\alpha))$.

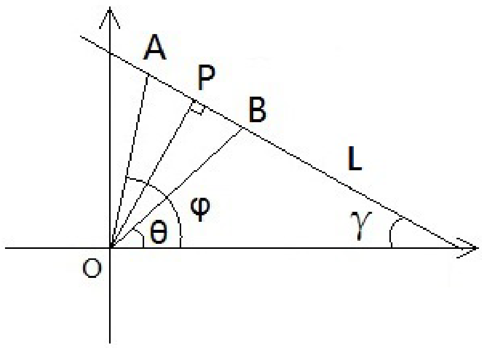

Figure 7. Diagram of any line after plane rotation

Before plane rotation, the angle γ between line L and X axis is calculated as follows.

$$\gamma = \arctan\left(\frac{A.y - B.y}{A.x - B.x}\right) = \arctan\left(\frac{OA \cdot \sin\phi - OB \cdot \sin\phi}{OA \cdot \cos\phi - OB \cdot \cos\phi}\right) = \arctan\left(\frac{\cos\left(\frac{\phi+\theta}{2}\right) \cdot \sin\left(\frac{\phi-\theta}{2}\right)}{-\sin\left(\frac{\phi+\theta}{2}\right) \cdot \sin\left(\frac{\phi-\theta}{2}\right)}\right) = \arctan\left(-\cot\frac{\phi+\theta}{2}\right) = \frac{\pi-(\phi+\theta)}{2} - \alpha$$

After plane rotation, the angle between line L and X axis is calculated as follows.

$$\gamma' = \arctan\left(\frac{A'_y - B'_y}{A'_x - B'_x}\right) = \arctan\left(\frac{OA \cdot \sin(\phi+\alpha) - OB \cdot \sin(\theta+\alpha)}{OA \cdot \cos(\phi+\alpha) - OB \cdot \cos(\theta+\alpha)}\right)$$

$$= \arctan\left(\frac{\cos\left(\frac{\phi+\theta+2\alpha}{2}\right)\cdot\sin\left(\frac{\phi-\theta}{2}\right)}{\sin\left(\frac{\phi+\theta+2\alpha}{2}\right)\cdot\sin\left(\frac{\phi-\theta}{2}\right)}\right)$$

$$= \arctan\left(\cot\left(\frac{\phi+\theta}{2}+\alpha\right)\right)$$

$$= \frac{\pi-(\phi+\theta)}{2}-\alpha$$

Thus, $\gamma-\gamma'=\alpha$.

Therefore, if the plane rotates at an angle α around any point on the plane, the angle for each line's rotation is still α.

(End of proof.)

This theorem ensures that the image taken at any observation point with any planar rotation angle can be corrected according to the rotation angle of any straight line in the image.

6. Rectification of rotation angle for the captured image

According to Theorem 2, the difference between the angle of line AD and the X axis in the captured image (θ) and the angle of line AD and the X axis in the standard image (θ) is the rotation angle of the image, i.e., α. By rotating the image in the opposite direction by the angle α, the captured image can be corrected to the standard image.

7. PMRS layer architecture

The PMRS realizes the visual display interface of the dial image and recognition results. The layer structure includes the background layer, data layer, message layer, menu layer, and image frame layer. The layer architecture is shown in Figure 8.

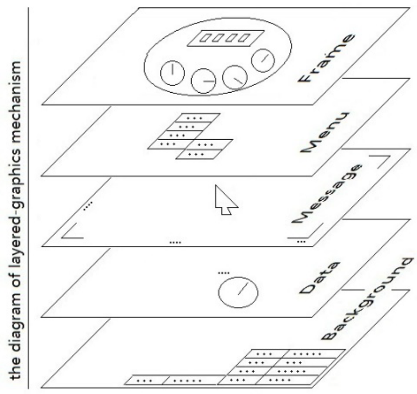

Figure 8. Layer architecture of PMRSIdentification algorithm flow

The process used by the PMRS to identify the dial position and scale is shown in Figure 9. The calculation process includes four steps: image preprocessing, dial position detection, dial scale detection, and dial rotation angle calculation.

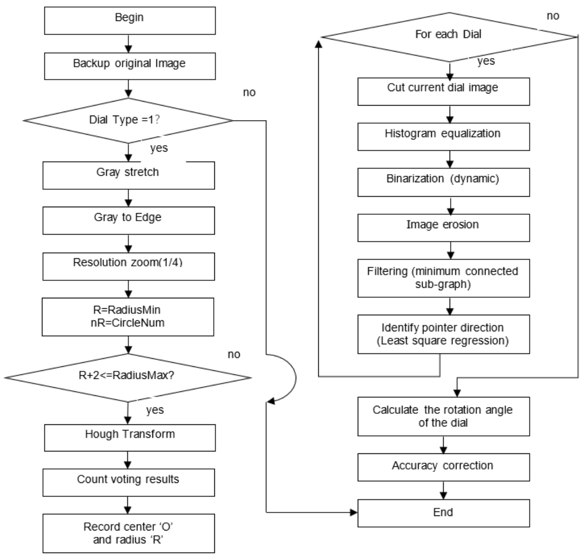

Figure 9. Flowchart of PMRS identifying dial position and scale value

8. System Computational Efficiency and Data Analysis

System computational efficiency

In practical applications, the angle of an image captured by a camera cannot be accurately controlled, which leads to uncertainty in the estimation of the rotation angle of the image. The PMRS is suitable for images captured from any angle. The multi-angle test result for a water meter using this system is shown in Figure 10.

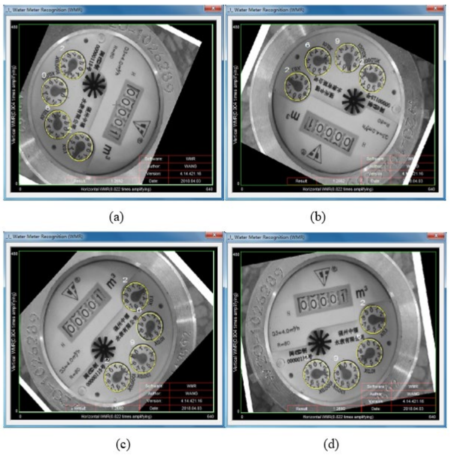

Figure 10. Detection effect of multi-angle photography for water meter image. (a) The snapshot image is rotated 115 degrees clockwise. (b) The snapshot image is rotated 205 degrees clockwise. (c) The snapshot image is rotated 315 degrees clockwise. (d) The snapshot image is rotated 350 degrees clockwise

In practical applications, the distance between camera and dial cannot be accurately controlled, which leads to uncertainty about the size of the dial in the image. The system is a self-adaptive PMRS for capturing distance. The zoom test effect of the system is shown in Figure 11.

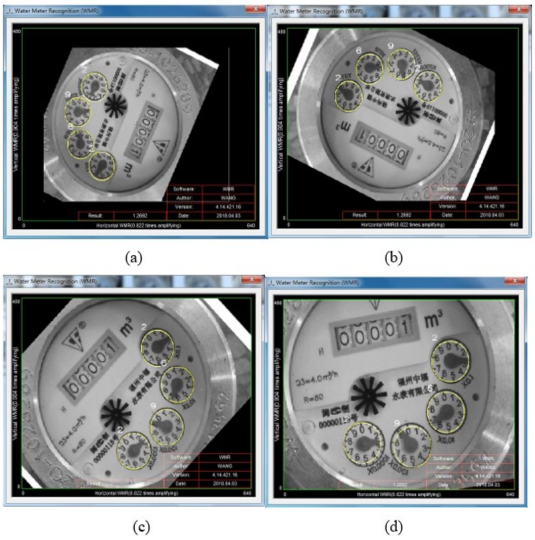

Figure 11. Effect chart of pointer meter image scaling test. (a) The image is rotated 115 degrees clockwise and reduced to 80% of the original size. (b) The image is rotated 205 degrees clockwise and reduced to 90% of the original size. c) The image is rotated 315 degrees clockwise and increased to 110% of the original size. (d) The image is rotated 350 degrees clockwise and increased to 130% of the original size

Experiments were conducted by contaminating meter images with Gaussian noise and impulse disturbance at different noise levels. The proposed PMRS method was tested under noisy image conditions, and dial localization and reading accuracy were evaluated. Experimental results show that PMRS maintains stable recognition performance under moderate noise contamination, with only gradual degradation at higher noise levels. This demonstrates that the proposed method has good robustness for practical industrial acquisition environments where sensor degradation may occur.

Table 1. Adaptive performance of PMRS under different image scaling conditions

Test Sample	Rotation Angle	Image Scale	Dial Detection	Pointer Recognition
Sample 1	115°	80%	Successful	Successful
Sample 2	205°	90%	Successful	Successful
Sample 3	315°	110%	Successful	Successful
Sample 4	350°	130%	Successful	Successful

These scaling conditions simulate long-distance and short-distance camera capture scenarios that result in apparent dial size variations. As shown in Table 1 the proposed PMRS successfully detected the dial region and recognized the pointer under all test conditions, demonstrating robustness to distance variation and confirming the adaptive capability of the improved Hough transform algorithm.

9. System test data analysis

During the design process of the PMRS, the group optimized the Hough transform algorithm, which identifies circles with different radii, and also improved the computational efficiency of the Hough transform for circle detection. Table 2 lists the theoretical computing times for three algorithms, the calculation process for which can be found in Section 2 of this paper. Table 3 lists the comparison results of computational efficiency for the improved Hough transform algorithm, Different dial configurations with varying dial density and overlap conditions were tested. The proposed PMRS method maintained high detection and reading accuracy even in clustered scenarios, with only slight increases in computational time as the number of dials increased. These results demonstrate that PMRS can effectively scale to dense multi-dial environments encountered in practical water meter systems Hough transform algorithm based on multi-resolution, and General Hough transform algorithm. the group added some system-call functions, such as GetTickCount, to the PMRS in order to obtain the statistics for algorithm time consumption, shown in Table 3 in milliseconds.

Table 2. Comparisons of computing times for the Hough-transforms improved by the group, Hough transform based on multi-resolution [2] [11], and the general Hough transform algorithms for detecting circles in water meter

	Computing times (million times)			
Samples	**Improved Hough transforms by the Group**		**Multi-resolution Hough transform**	**Generalized Hough transform**
	Pass 1	**Pass 2**		
Water meter (640 × 480 resolution, dial diameter about 80 pixels with 16 pixels fluctuation range)	56	1	112	1800

Note: Pass1 in the table 1 represents the computing times consumed by the improved algorithm in macro data processing, and Pass2 in the table 1 represents the computing times consumed by the improved algorithm in micro data processing.

Table 3. Comparisons of computing efficiency between the Hough-transform improved by the group, Hough transform based on multi-resolution [11] and the Generalized Hough transform algorithms [2] for detecting circles in water meter

	Computing efficiency (millisecond)			
Samples	**Improved Hough transforms**		**Multi-resolution Hough transform**	**Generalized Hough transform**
	Pass 1	**Pass 2**		
Sample 1	820	15	1632	24441
Sample 2	825	15	1649	24549
Sample 3	831	16	1688	24783
Sample 4	826	15	1669	24679

Note: Pass1 in Table 2 represents the time consumed by the improved algorithm in macro data processing, and Pass2 in Table 2 represents the time consumed by the improved algorithm in micro data processing. Different gain coefficient values were tested for small-, medium-, and large-radius dial configurations, and localization precision was evaluated using centre coordinate error. Results indicate that very low gain coefficients lead to insufficient voting concentration, whereas excessively high values amplify local noise responses. A moderate gain coefficient provides stable Hough voting localization precision across different dial radii, demonstrating the robustness of the proposed initialization strategy.

Through the comparative analysis shown in Table 2, it can be concluded that the computational efficiency of the improved Hough transform algorithm the group proposed is approximately twice that of the Hough transform based on multi-resolution.

The pointer direction estimated by PMRS was compared with manually annotated reference angles. Least-squares pointer-line modelling was used to fit the detected pointer trajectory, and the angular deviation was calculated as the absolute difference between estimated and reference pointer angles. Experimental results showed that PMRS maintained low angular estimation error while achieving faster computational performance, demonstrating that the proposed method improves both efficiency and meter reading precision.

Table 4. Benchmark Comparison of PMRS with Conventional Circle Detection Methods

Method	Average Runtime (ms)	Recognition Robustness	Remarks
PMRS (Improved Hough Transform)	840.75	High	Adaptive to distance and angle
Canny + Circular Least-Squares Fitting	1100–1300	Moderate	Sensitive to noise and incomplete edges
Multi-resolution Hough Transform	1659.50	High	Higher computation
Generalized Hough Transform	24613.00	High	Highest computation

Although edge-based fitting methods can provide efficient circle approximation under ideal imaging conditions, their performance is more sensitive to edge discontinuity, noise, and shooting angle variations. In contrast, PMRS maintains robust dial localization through constrained Hough-based voting and adaptive geometric correction, providing improved reliability for pointer meter recognition under practical image acquisition conditions is shown in Table 4.

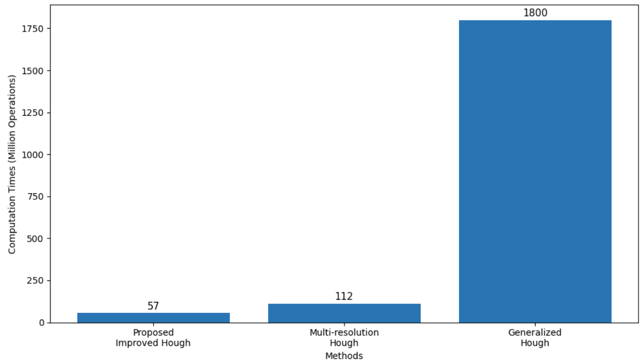

Figure 12. Comparison of theoretical computational complexity among the proposed improved Hough transform, multi-resolution Hough transform, and generalized Hough transform methods

Figure 12 presents the theoretical computational complexity comparison of three circle-detection algorithms. The proposed improved Hough transform requires approximately 57 million operations, while the multi-resolution Hough transform requires 112 million operations, and the generalized Hough transform requires approximately 1800 million operations. The graphical comparison clearly demonstrates that the proposed method significantly reduces computational complexity. Compared with the multi-resolution Hough transform, the proposed algorithm reduces computational cost by nearly 50%, while compared with the generalized Hough transform, the computational complexity is reduced by more than 30 times.

The mean runtime, standard deviation, and 95% confidence interval were calculated to quantify statistical variation. Results indicate that PMRS maintains stable computational performance with narrow confidence intervals, demonstrating consistent execution efficiency across repeated observations.

The proposed PMRS framework within the current instrument recognition landscape, a comparative analysis was conducted against representative contemporary deep learning meter-reading architectures, including CNN-based regression, YOLO-based recognition, and U-Net segmentation methods [29-30]. Deep learning approaches generally achieve high recognition accuracy due to their strong feature-learning capability; however, they require extensive training datasets, larger model sizes, and higher computational resources. In comparison, the proposed PMRS framework achieves competitive meter-reading accuracy while maintaining significantly lower runtime and computational overhead. Unlike deep learning models, PMRS does not require training or parameter-intensive optimization, making it more suitable for lightweight industrial deployment and resource-constrained embedded environments. Experimental comparison indicates that although deep learning methods offer strong generalization performance, PMRS provides a practical balance of accuracy, efficiency, and implementation simplicity, demonstrating its competitiveness as a handcrafted alternative for industrial meter recognition applications.

10. Summary

Automatic recognition technology for pointer meters is an important topic and technological frontier in the field of pattern recognition [21][31]. This paper expounded the mathematical principle of the pointer meter recognition algorithm and put forward two theorems for pointer meter recognition, which are the theorem of left-right positional relationship between two points on the plane (theorem 1) and the theorem of invariable rotation angle on the plane (theorem 2). According to these two theorems, the group designed the PMRS, which is adaptive to rotation of the captured image by any angle [32]. The system was demonstrated to provide a long-distance and short-distance self-adaptive function of pointer meter recognition through an improved Hough transform algorithm. In addition, the research group made appropriate modifications to the formula of Hough transform to reduce the gain value of the algorithm and improve computational efficiency. Compared with the standard Hough transform algorithm, computational efficiency is improved by more than 16-fold. The computational efficiency is almost twice that of the Hough transform algorithm based on multi-resolution. The experimental results also prove that computational efficiency decreases from 1.6 s to less than 1 s when the algorithm is used to detect water meter instruments. This computational efficiency puts the time delay of recognition within a user-tolerated range. The improved Hough transform algorithm proposed in this article is based on the detection of circles. To apply this algorithm to detect other shapes, appropriate modifications to the algorithm model are required. In addition, for circles with different radii, this paper proposes a detection algorithm that uses the improved Hough transform multiple times, so the algorithm still has computational redundancy, which is also a sustainable improvement of the algorithm.

Funding Statement

This work is supported by the following projects.
Key Preresearch Topics of North China Institute of Aerospace Engineering (ZD201703);
Langfang Science and Technology Project (2017011023);
Funded by Science and Technology Project of Hebei Education Department (ZD2019138);
Defense Industrial Technology Development Program（JCKY201907D004);
S&T Program of Hebei（D2020409005).

Acknowledgments

We would like to thank Editage (www.editage.cn) for English language editing.

Data Availability Statement

All data, models, and code generated or used during the study appear in the submitted article.

Conflicts of Interest

The authors declare that there is no conflict of interest regarding the publication of this paper.

References

[1] Zhou D, Yang Y, Zhu J, Wang K. Intelligent reading recognition method of a pointer meter based on deep learning in a real environment. Measurement Science and Technology. 2022 May 1;33(5):055021.

[2] Wang C, Pei H, Tang G, Liu B, Liu Z. Pointer meter recognition in UAV inspection of overhead transmission lines. Energy Reports. 2022 Aug 1;8:243-50.

[3] Kassim AA, Mian Z, Mannan MA. Connectivity oriented fast Hough transform for tool wear monitoring. Pattern Recognition. 2004 Sep 1;37(9):1925-33.

[4] Wang J, Li H, Bai B. A novel method of automatic reading for rotor water meter based on image processing. International Journal of Simulation and Process Modelling. 2022;18(1):77-85.

[5] Pei, L. Q., & Huang, Q. D. (2016). Development of automatic verification for high precision pointer instrument based on machine vision. *Measurement & Control Technology, 35*(9), 153–156

[6] Qu, R. J., Xu, Z. Z., & Zhang, Y. J. (2012). Embedded environment fast pointer meter analysis algorithm research. *Software, 33*(8), 138–143.

[7] Sun, Y. H. (2015*).* Research on recognition system of pointer meter reading based on machine vision (Master's thesis). Jilin University.

[8] Chen XY, Wang Q, Li BL. Improved hough algorithm for circle detection. Computer Systems & Applications. 2015;24(8):197-9.

[9] Lee J, Park M, Eo I, Koo B. An X-band FMCW radar for detection and tracking of miniaturized UAVs. In2017 International Conference on Computational Science and Computational Intelligence (CSCI) 2017 Dec 14 (pp. 1844-1845). IEEE.

[10] Zhang K, Zuo W, Chen Y, Meng D, Zhang L. Beyond a gaussian denoiser: Residual learning of deep cnn for image denoising. IEEE transactions on image processing. 2017 Feb 1;26(7):3142-55.

[11] Tang Q, Tang C, Zhang H. An improved accurate circle detection method based on hough transform. Aeronautical Computing Technique. 2017;47(03):58-61.

[12] Lei T, Jia X, Liu T, Liu S, Meng H, Nandi AK. Adaptive morphological reconstruction for seeded image segmentation. IEEE Transactions on Image Processing. 2019 Jun 7;28(11):5510-23.

[13] Badrinarayanan V, Kendall A, Cipolla R. Segnet: A deep convolutional encoder-decoder architecture for image segmentation. IEEE transactions on pattern analysis and machine intelligence. 2017 Jan 2;39(12):2481-95.

[14] YUE DX, HUANG XS. Method of Line Detection Based on Improved Multiresolution Hough Transform. Computer Simulation. 2006;9.

[15] Cheng Y, Wang Y, Zhang D, Zhang Z. Recognition of partially occluded objects based on generalized Hough transform. JOURNAL-CHINA UNIVERSITY OF SCIENCE AND TECHNOLOGY. 1997;27:411-8.

[16] Pare S, Bhandari AK, Kumar A, Singh GK. An optimal color image multilevel thresholding technique using grey-level co-occurrence matrix. Expert Systems with Applications. 2017 Nov 30;87:335-62.

[17] Xue Z, Du P, Li J, Su H. Sparse graph regularization for hyperspectral remote sensing image classification. IEEE Transactions on Geoscience and Remote Sensing. 2017 Jan 16;55(4):2351-66.

[18] Shao Y, Sang N, Gao C, Ma L. Spatial and class structure regularized sparse representation graph for semi-supervised hyperspectral image classification. Pattern Recognition. 2018 Sep 1;81:81-94.

[19] Luo F, Huang H, Liu J, Ma Z. Fusion of graph embedding and sparse representation for feature extraction and classification of hyperspectral imagery. Photogrammetric Engineering & Remote Sensing. 2017 Jan 1;83(1):37-46.

[20] Cakir F, He K, Bargal SA, Sclaroff S. Hashing with mutual information. IEEE transactions on pattern analysis and machine intelligence. 2019 May 3;41(10):2424-37.

[21] Han SC, Xu ZY, Yin ZC, Wang JX. Research review and development for automatic reading recognition technology of pointer instruments. Computer Science. 2018;45(S1):54-7.

[22] Zhang Q, Bao X, Wu B, Tu X, Jin Y, Luo Y, Zhang N. Water meter pointer reading recognition method based on target-key point detection. Flow Measurement and Instrumentation. 2021 Oct 1; 81:102012.

[23] Bingjie T, Jiale H, En LI. An Applied Method for Reading Recognition of Index-instrument [J]. Opto-Electronic Engineering. 2011;38(04):145-50.

[24] Zhou, W. (2006). Research on pointer meter recognition system based on computer vision (Master's thesis). Zhejiang University

[25] Chen, R. (2006). Research and development of high precision instrument automatic verification system based on digital image processing technology *(Master's thesis).* Shandong University of Technology.

[26] Stasiak, K., Ciesielski, M., Samczynski, P., & Gromek, D. (2019). Preliminary results of drone's propellers detection using K-band and mm-wave FMCW radar. *20th International Radar Symposium (IRS)*.

[27] Zhang M, Yu Z, Zhu J. Research of Algorithm for Bitmap's Vectorization.

[28] Al-Emadi S, Al-Ali A, Mohammad A, Al-Ali A. Audio based drone detection and identification using deep learning. In2019 15th International Wireless Communications & Mobile Computing Conference (IWCMC) 2019 Jun 24 (pp. 459-464). IEEE.

[29] Ismael AA, Baykara M. Digital Image Denoising Techniques Based on Multi-Resolution Wavelet Domain with Spatial Filters: A Review. Traitement du Signal. 2021 Jun 1;38(3):639.

[30] Feng, H., & Li, C. (2023). Research on automatic recognition algorithm of instrument reading based on image processing. *Automation Application, 64*(13), 193–195.

[31] Zhang J, Liu W, Xu S, Zhang X. Key point localization and recurrent neural network based water meter reading recognition. Displays. 2022 Sep 1;74:102222.

[32] Zhang, Y. (2023). Intelligent edge caching and computing for scalable information systems. *EAI Endorsed Transactions on Scalable Information Systems*, *10*(5).